




Phytochemicals of “Magahi Pan” (*Piper betle* L. var. *magahi*) as Potential H^+/K^+ -ATPase Inhibitors: In-Silico Study and ADME Profile

Singh Nadkar Narayan Singh^{1*} , Gurfateh Singh¹, Alok Mukherjee², Sailendra Kumar Mahanta³, Shivnath Das⁴

¹Department of Pharmacognosy, University School of Pharmaceutical Sciences, Rayat- Bahra University, Mohali, Panjab, India.

²Department of Pharmacognosy, United Institute of Pharmacy Prayag Raj, Uttar Pradesh, India.

³Department of Pharmaceutical Sciences, School of Pharmacy, the Assam Kaziranga University, Assam, India.

⁴Department of Agronomy, Betel Vine Research Institute, IslamPur, Bihar, India.

Abstract

Background and objectives: In India, peptic ulcer is most prevalent gastrointestinal disease. Historically *Piper betle* has been used to treat stomach problems. In order to identify the phytochemicals present in *Piper betle* L. var *magahi* LC/MS spectroscopic analysis was performed, following which, potential phytomolecules with H^+/K^+ -ATPase inhibitory activity were chosen using in-silico evaluation. **Methods:** Phytochemicals in ‘Magahi pan’ were investigated and potential H^+/K^+ -ATPase inhibitor phytochemicals that were screened through in-silico analysis and ADME profile of selected phytochemicals were evaluated. Phytochemical characterization was done with the help of LC/MS followed by molecular docking against enzyme H^+/K^+ -ATPase (PDBID:5YLV) using Autodock4.2 and Swiss ADME. The binding affinity, free energy, physicochemical property, saturation of carbon atoms, number of hydrogen bond acceptors-donors, molar refractivity, lipophilicity, water solubility, and drug likeness property were evaluated in-silico for their predicted bioactivity against H^+/K^+ -ATPase. **Results:** A total of 67 phytoconstituents were identified through LC/MS positive and negative ionization mode spectral analysis and six were selected on the basis of binding energy. Molecular docking results revealed that the isolated compounds interacted with target protein H^+/K^+ -ATPase with minimum binding energy ranging from (1) netilmicin (-9.29 kcal/mol); (2) benzotropine (-9.07 kcal/mol); (3) 5,6,7,3',4' pentahydroxyisoflavone (-8.45 kcal/mol); (4) 2-O-acetylpsuedolycorine (-8.02 kcal/mol); (5) R-95913 (-7.73 kcal/mol) and (6) luteolin (-6.93 kcal/mol), respectively. **Conclusion:** The ADME profile analysis and docking studies revealed 5,6,7,3',4' pentahydroxy-isoflavone and luteolin as potential molecules for inhibiting H^+/K^+ -ATPase.

Keywords: H^+/K^+ -ATPase inhibitors; Magahi pan; molecular docking; peptic ulcer; *Piper betle*

Citation: Singh Nadkar Narayan S, Singh G, Mukherjee A, Kumar Mahanta S, Das S. Phytochemicals of “Magahi pan” (*Piper betle* L. var. *magahi*) as potential H^+/K^+ -ATPase inhibitors: in-silico study and ADME profile. Res J Pharmacogn. 2023; 10(3): 61–75.

Introduction

Peptic ulcer is a significant medical issue that includes both gastric and duodenal ulcers and has been a significant global challenge. The prevalence of peptic ulcer is higher in the elderly

population, with the highest incidence observed between the ages of 55 and 65. Duodenal ulcers are more common in men than gastric ulcers, while the opposite is true for women [1]. The role

* Corresponding author: 18-m-2434@rayatbahrauniversity.edu.in

of acid in peptic ulcer disease has gained global acceptance since the introduction of proton pump inhibitors (PPIs) as the main therapeutic approach. However, long-term use of PPIs and antibiotics can lead to serious side effects, including cancer. Synthetic drugs used to treat peptic ulcer also have unwanted side effects [2]. Studies have shown that PPIs can induce tumors in the liver, gallbladder, and pancreas by affecting the duodenal and biliary tract microbiome. Hepato biliary pancreatic cancer (HBPC) tumor has poor prognosis than other types of cancer and is difficult to treat. Even normal doses of PPIs have been linked to HBPC. Therefore, there is a need for the discovery of non-toxic, cost-effective treatments for peptic ulcer. [3].

“Magahi pan” (*Piper betle* L. var. *magahi*) is a member of the Piperaceae family and is cultivated in Magadh region, presently spreads from Aurangabad, and Gaya, districts of present Bihar. This vine is popularly used as a mouth freshener agent and is also used in the treatment of gastrointestinal disorders and dental problems in large rural societies. The local people's varied uses of this vine sparked an interest in exploring its phyto-constituents and potential pharmacological benefits. Moreover, this vine has shown to have anticancer, antibacterial, antifungal, gastro-protective, anti-diabetic, anti-oxidant, wound-healing, anti-asthmatic, anti-malarial, insecticidal, anti-allergenic, anti-protozoal, and anti-biofouling activity [4-19]. The present research was aimed to evaluate and characterize the phytoconstituents of the ethanol extract of dried leaves of *Piper betle* L. var. *magahi* and its in-silico evaluation for therapeutic benefit in ulcers. This study is the first of its kind to investigate the phytoconstituents of “Magahi pan” through LC/MS spectroscopic analysis by negative and positive ionization modes and its potential to treat peptic ulcers.

It is reported by various researchers that the biological activity of various cultivar of *Piper betle* is due to the flavonoids and phenolic compounds present in the drug [20]. LC/MS is used for characterization and quantifying a wide variety of complex samples, and it is a globally accepted technique in the determination of phytochemicals in complex plant extracts [21]. In this regard, the present study established and validated a rapid and sensitive LC/MS spectroscopic analysis.

The in-silico study comprises molecular docking study followed by ADME profiling of selected phytoconstituents. The design of new drugs is greatly influenced by molecular docking methodologies, which aim to predict the experimental binding mode and affinity of a small molecule in the binding site of the receptor target of interest. The three main connected goals of molecular docking include pose prediction, virtual screening, and binding affinity estimation [22]. Quantitative-structure-property relationships (QSPRs), which connect structural information to physical and chemical characteristics or even biological behavior. Quantitative structure activity relationship (QSAR), are used in in-silico and ADME prediction to develop tools and models based on experimental data to predict in vivo behavior of compounds. Gained empirical data are then related to descriptors/properties thereby supporting the process of hit-to-lead optimization [23].

Material and Methods

Ethical considerations

The Ethics committee of United Institute of Pharmacy Naini Prayagraj Uttar Pradesh approved this research with code of 1451/PO/Re/S/11/CCSEA.

Plant material

The leaves of *Piper betle* L., “Magahi pan”, were procured from the Magahi Pan Research Institute Islampur Nalanda (Bihar), India in July 2021. The plant was authenticated by Dr. Shivnath Das, a senior scientist in the Magahi Pan Research Institute, Islampur Nalanda (Voucher specimen no. T- 01512).

Extraction

For obtaining the ethanol extract, the leaves were washed with tap water and then dried in a hot air oven at 40 °C for two days. The dried leaves were ground into powder. Powered leaves (100 g) were subjected to continuous Soxhlet extraction with ethanol for 10 h. The ethanol extract was filtered using Whatman filter paper (No. 1) and then dried. It was further used for liquid chromatography and mass spectroscopy (LC/MS) spectroscopic analysis.

LC/MS analysis through positive and negative ionization mode

The ethanol extract of “Magahi pan” was

subjected to liquid chromatography along with mass spectroscopy (LC/MS) using Agilent Q-ToF G6540B connected to Agilent 1260 Infinity II HPLC system. The details of method used in LC/MS analysis is given in Table 1.

Table 1. Method details of liquid chromatography and mass spectroscopy (LC/MS)

Parameters	Value	
Column	Agilent Zorbax, 2.1 X 50mm, 1.8µm	
Column Temperature	40 °C	
Mobile Phase A	0.1% formic acid in water	
Mobile Phase B	0.1% formic acid in acetonitrile	
Mobile Phase Flow Rate	0.3 mL/min	
Chromatographic gradient		
Time (min)	% Mobile phase A	% Mobile phase B
0	95	5
18	5	95
27	5	95
27.1	95	5
30	95	5
Mass Spectroscopy		
MS Ion source	Dual AJS ESI	
Polarity	Negative and Positive	
MS Scan range	At m/z 60 to 1600	
Ion source Parameters		
Nebulizer Gas Temperature	350 °C	
Sheath Gas Temperature	300 °C	
Drying gas	8.1 /min	
Nebulizer Gas	40 psig	
Sheath Gas Flow	101 /min	
Capillary Voltage	2500 V	
Nozzle Voltage	500 V	

Molecular docking study

The molecular docking study was conducted using Autodock 4.2 package. Crystal structures of the gastric proton pump-the H⁺/K⁺-ATPase (PDB:5YLV) were obtained from <https://rcsb.org>, while 3D structures of various chemical constituents present in “Magahi pan” were downloaded from PubChem [24]. The chemical constituents identified were then docked into the protein active site. Energy minimization was carried out with the Autodock 4.2 module to perform geometry optimization calculations for the chemical constituents identified from “Magahi pan”.

ADME and pharmacokinetic predictions

After the molecular docking study, the absorption, distribution, metabolism and elimination (ADME) of six selected phytoconstituents were screened using online tool ‘<http://www.swissadme.ch/>’. Swiss ADME is a comprehensive website

recently launched by the Swiss Institute for Bioinformatics (SIB) with the aim to evaluate the ADME parameters of drug candidates and molecules and provide information that enables preliminary uncertainty determination in the drug discovery process.

The input zone of the Swiss-ADME web tool includes a molecular sketcher based on Chem Axon's Marvin JS, which enables users to draw and edit 2D chemical structures [25]. These structures are then transferred to the right-hand side of the submission page, which serves as the actual input for computation. The list is structured to contain one input molecule per line entry system, known as SMILES. Complete results are available in tables, graphs, and spreadsheets. Swiss ADME is a platform used to determine the Lipinski rule of five for drug likeness of oral bioavailability, which is a composite harmony of molecular properties (electronic distribution, hydrophobicity, hydrogen bonding characteristics, molecular flexibility, size and constitutional appearance that determines whether an unknown molecule is similar to a known drug.

Result and Discussion

Negative ion mode mass spectroscopy is the most commonly used tool in phyto-analysis. The electrons spray process produces (M-H⁻) ions for the determination of the mass to charge ratio of the sample molecules. Electrospray ionization (negative ionization mode) has been employed to determine lower ketones and carboxylic acid derivatives [26]. Twenty phyto-constituents have been identified by negative ionization mode by comparing, peak, retention time, peak area and peak height (Figure 1A). In mass spectroscopy, positive ionization involves the formation of positive ions in order to determine the mass-to-charge ratio of the sample molecule. Positive ionization is designated as the [M+H⁺]. In this process positive ions are created, and it is utilized in the determination of the mass-to-charge ratio of the molecule under analysis [27]. In this technique, ions in high yield are detected as compared to negative ionization mode. Forty-seven phytoconstituents have been identified by this mode in ethanol extract of “Magahi pan” (Figure 1B).

The compounds detected using positive and negative ionization modes were categorized into two main groups: nitrogenous and non-nitrogenous compounds (supplementary Table 1

and 2) (supplementary Figure 1). While the majority of nitrogenous compounds were identified using positive ionization mode, only one nitrogen-containing compound, ticarcillin, was detected using negative ionization mode. The LC/MS study revealed that a significant number of compounds were detected using positive ionization mode.

The binding energy is the change in the free energy associated with binding process. The magnitude of the binding energy is a measure of how strong the interaction exists between the ligand and the protein and hence it is often directly related to the potency of the ligands [28]. LC/MS spectroscopic analysis identified 67 phytochemicals of which six phytochemicals were screened on the basis of binding energy against enzyme H^+/K^+ -ATPase (protein ID: 5YLV) (Table 2).

Netilmicin showed the highest binding energy (-

9.29 kcal/mole) among all, this phytomolecule showed maximum receptor specificity. The next phytomolecule, benztropine, was reported to be highly selective (-9.07 kcal/mole). The third phytomolecule was screened with (-8.45 kcal/mole) and identified as 5, 6, 7,3',4' pentahydroxyisoflavone. The fourth one was 2-O-acetylpsudolycorine (-8.02 kcal/mole), while the fifth one was R-95913 (-7.73 kcal/mole). The last one, luteolin, (-6.93 kcal/mole), was selected on the basis of binding energy.

The inhibitory constant is the concentration required to produce half maximum inhibition between ligands and enzyme. It is an indication of how much the ligand is potent. The smaller the inhibitory constant the greater is the potency. Nowadays, inhibitory constant is being reported by various drug companies to prove the potency of the drug molecules [29].

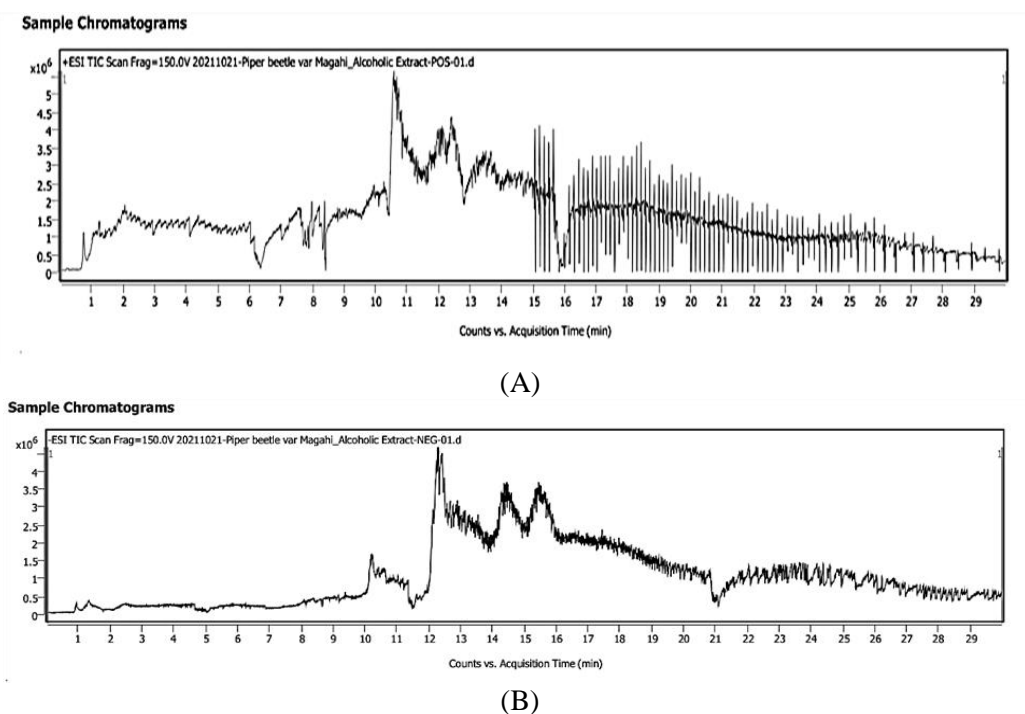


Figure 1. Total electron ionization chromatogram of “Magahi pan” ethanol leaves extract by negative ionization mode (A) and positive ionization mode (B)

Table 2. Estimated binding energy and inhibition constant value of six selected phyto molecules

PubChem ID	Phyto molecules name	Estimated binding energy (Kcal/mole)	Ki value
19919505	R-95913	-7.73 kcal/mol	-2.17 μ M
443726	2-O-Acetylpsudolycorine	-8.02 kcal/mol	-1.32 μ M
441306	Netilmicin	-9.29 kcal/mol	-156.18 nM
10733103	5,6,7,3',4' Pentahydroxy isoflavone	-8.45 kcal/mol	-635.89 nM
120549	Benztropine	-9.07 kcal/mol	-225.99 nM
5280445	Luteolin	-6.93 kcal/mol	-8.34 μ M

The Ki value of netilmicin, benzotropine and 5, 6, 7, 3', 4' pentahydroxyisoflavone was (156.18 nM), (225.99 nM) and 635.89 nM, respectively.

The Ki values of all these three phytomolecules are in nano range that indicate their potency. The fourth molecule 2-O-acetylpsedolycorine reported (1.32 μM). The fifth phytomolecule R - 95913 and sixth luteolin reported 2.17 μM and 8.34 μM, respectively (Table 2).

The docking process was followed by the identification of the amino acid residue present at the binding site. This would help to understand the confirmation of the binding site was either same or different for the selected ligands. The 2D and 3D interaction analysis was performed with the help of discovery studio visualizer to identify the binding site and its amino acid residue which is depicted in (Figure 2). The details of amino acids and type of interactions between the binding site of H⁺/K⁺ -ATPase enzyme and ligand given have been shown in supplementary Table 3.

The color of the surface vertices in Figure 3 is derived from the classification of the atom covered by the surface as either a hydrogen bond donor or acceptor. If an atom was a hydrogen bond donor, the atom was assigned a fictitious charge of +1. If an atom was hydrogen bond acceptor the atom was assigned a fictitious charge of -1. The default color spectrum used was green, white and magenta. The full color map range of value was -1.0 to +1.0. Negative value (green) corresponded to hydrogen bond acceptors whereas positive values, (magenta) corresponded to hydrogen bond donors. Hydrogen bonding explains topographical analysis of the binding place that would highlight the density of hydrogen bond donors and acceptors present at the binding position [30]. The topographical analysis showed the presence of high density hydrogen bond acceptors compared to hydrogen bond donors at the binding place. The hydrogen bond is one of the most important classes of molecular interaction in biological systems, in case of ligand 2-O-acetylpsedolycorine the number of hydrogen bond acceptors was 6 and the number of hydrogen bond donors was 2. However, hydrogen bonds conferred directionality and specificity to the intramolecular interactions in these structures. This interaction is particularly important for proteins, where hydrogen bonds provide the organization for distinct folds and also provide the selectivity in the protein ligand

interaction that underlines molecular recognition at binding place. The hydrophobic effect provides the thermodynamic drive for the overall structure of nucleic acids, proteins, and membrane in water through the burials of hydrophobic groups and exposure of the hydrophilic groups. However, this interaction is particularly important for proteins, where hydrogen bonds provide the organization for distinct folds and also provide the selectivity in the protein ligand interaction that underlines molecular recognition at atomic levels. The details of hydrogen bond donors and acceptors, Vander wall interaction, Pi-alkyl interaction, Pi-anion interaction of above mentioned ligands are given in supplementary Table 3.

The atoms covered by the surface, which are part of amino acid residues, were attributed to aromatic ring edge/face and are depicted in Figure 4. For each aromatic ring, the ring center and ring normal were calculated. The default color spectrum used was blue, white and orange. Negative value (blue) corresponds to the edge of the aromatic ring whereas positive value (orange) corresponds to the face of the aromatic rings. Most of the amino acids possess aromatic side chains, so it becomes important to know the interaction between them [31].

The full color map range of values was -1.0 to +1.0. With the ligands 2-O-acetylpsedolycorine there were 24 aromatic heavy atoms which was highest among all. Details of aromatic heavy atoms associated with ligands are given in supplementary Table 3. Interpolated atomic partial charges between receptor and ligands are given in Figure 5. In this case, the charges q used, are the partial charges assigned to each atom covered by the surface. If no partial charges were available, the Gasteiger charge was calculated [32]. The default color spectrum used was red, white and blue. The full color map ranged from value -1.0 to +1.0. Values less than -0.1 were mapped to the color red and values larger than +0.1 were mapped to color blue. The fraction of carbon sp³ saturation was 0.39% with the ligand R-95913 and molar refractivity was 92.34 which indicated the volume of the molecule. As it is well established, molar refractivity is linked with the London dispersive force and drug receptor interactions [33].

In the case of ligand 2-O-acetylpsedolycorine, the fraction of carbon sp³ saturation was 0.50 and the molar refractivity was 90.59.

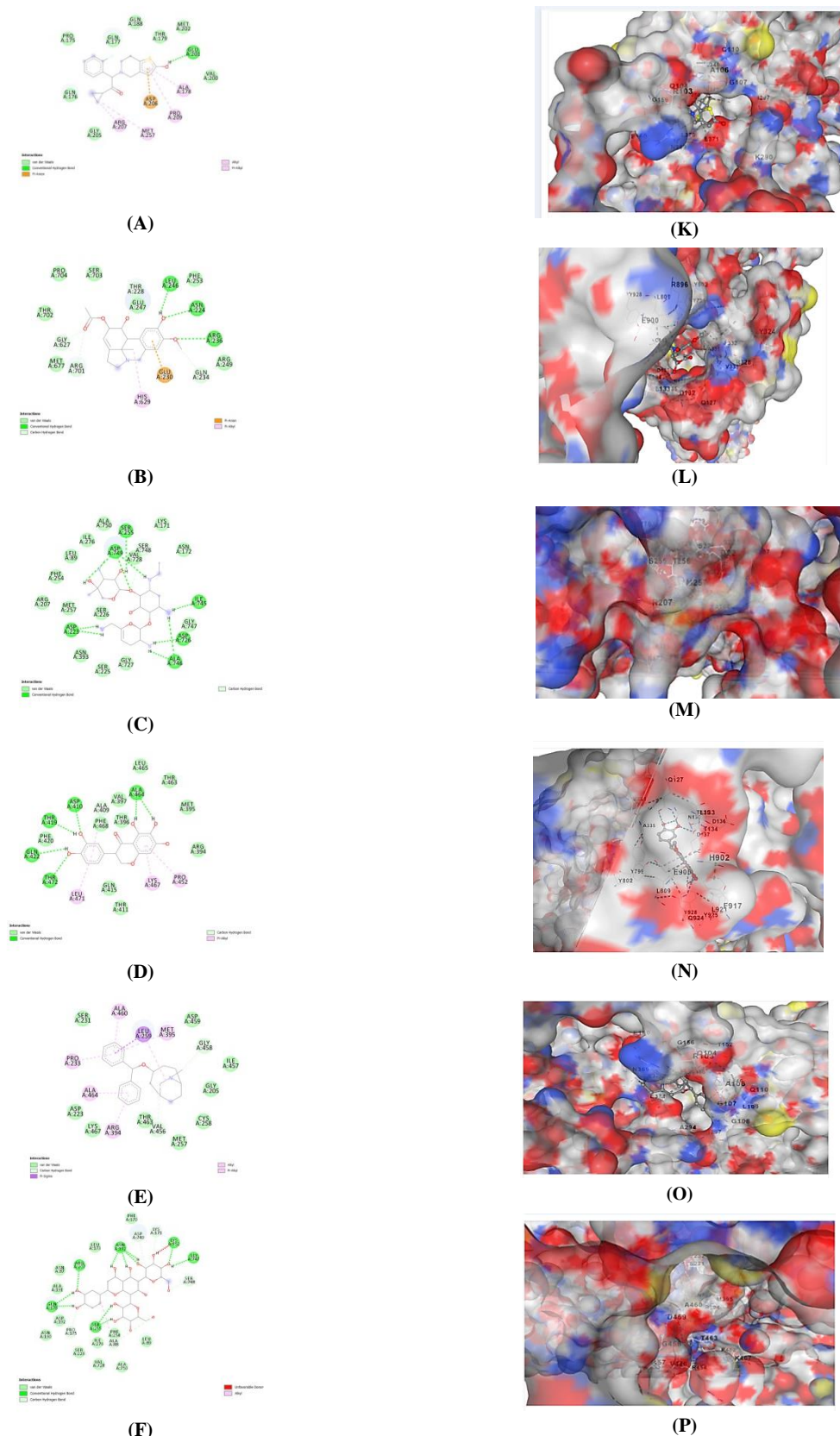


Figure 2. 2D interaction between ligands and enzyme H⁺/K⁺-ATPase enzyme (A) R-95913 (B) 2-O-acetylpsudolycorine (C) netilmicin (D) 5,6,7,3',4' pentahydroxyisoflavone (E) benztropine (F) luteolin , and from figure (K) to (P) illustrate 3D interactions

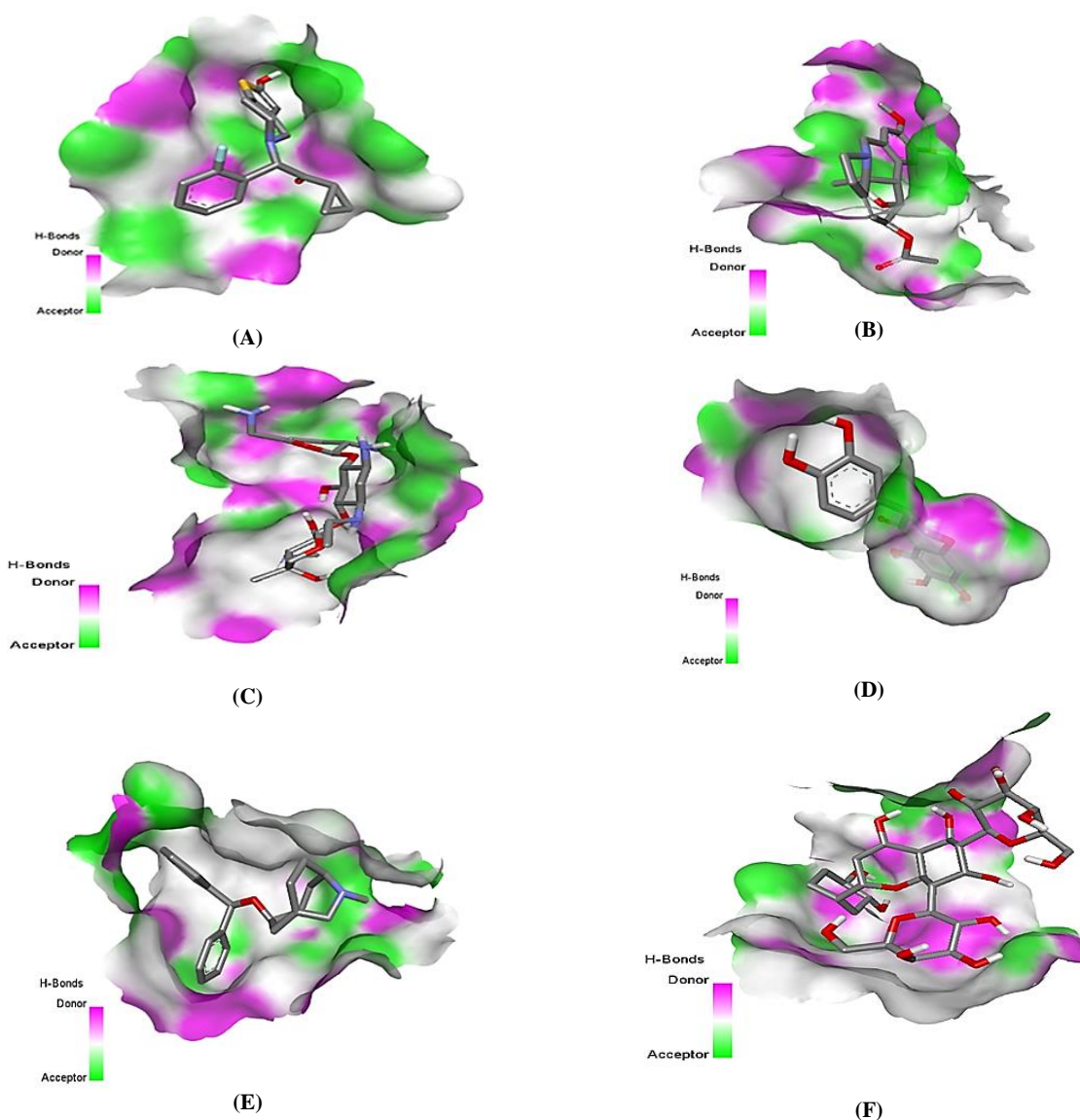


Figure 3. Three dimensional structure analysis of H⁺/K⁺-ATPase enzyme and ligands with respect to hydrogen bonding (A) R-95913 (B) 2-O-acetyl pseudoglycorine (C) netilmicin (D) 5,6,7,3',4', pentahydroxyisoflavone (E) benztropine (F) luteolin

The fraction of the carbon sp³ saturation in case of ligands netilmicin was 0.91 and molar refractivity was 128.32, which indicated size of the molecule. The fraction of the carbon sp³ saturation in the case of the 5, 6, 7, 3', 4' pentahydroxyisoflavone was 0.13 and the molar refractivity was 75.62. The fraction of the carbon sp³ saturation in the case of the ligand benztropine was 0.45 and molar refractivity was 102.83. The fraction of the carbon sp³ saturation in case of the ligands luteolin was 0.00 and molar refractivity was 76.01. The details of carbon saturation and molar refractivity of ligands is given in supplementary Table 3.

Within all amino acids, both the carboxylic acid functional group (C-terminus) and the amine functional group (N-terminus) got ionized after interactions with ligands. The ionizability characteristics of H⁺/K⁺-ATPase enzyme with ligands are depicted in Figure 6. The procedure to arrive at the color of the surface vertices was analogous to the procedure described for the hydrogen bond donor/acceptor. Fictitious charges were assigned to heavy atoms covered by the receptor surface that were also part of the amino acid residue [34]. The default color spectrum used was red, white and blue. The full color map range of values was -1.0 to +1.0. A negative

value (red) represented acidic residue, while a positive value (blue) represented basic residue. In the above ligand receptor complexes, the presence of amino acid aspartate (AASP206) and glutamate (AGLU201) explains the red color of the acidic residue at the binding site. The reasoning of blue color can be well explained with the presence of amino acid arginine and lysine with the ligand 2-O-acetylpsuedolycorine and receptor protein. As shown, the blue color is dominant in case of ligand netilmicin and receptor protein complex due to arginine, lysine and histidine amino acids at the binding site. The amino acid arginine and lysine along with ligands benztropine and receptor protein are responsible for blue color. Computer graphics also support the scientific data. The amino acid arginine can explain the presence of blue color at the binding site of ligand luteolin and receptor protein complex. Details of amino acids present at binding site and type of interaction between

receptor and ligand is given in supplementary Table 3. This concept was first introduced in 1971. Solvent accessible surface has been widely used in the analysis of protein structure and stability of ligand receptor complexes. Solvent accessibility surface property with ligands is well depicted in Figure 7.

For each specific atom within the surface covered by the residue, the relative residue solvent accessibility value (denoted as V) is calculated and assigned to the atom. This process allows for the determination of the accessibility of the residue to the solvent, providing valuable information about its interaction with the surrounding environment. [35]. The final color of a surface vertex was then obtained by mapping the value V of the atom closest to the surface vertex. Atoms with a distance of more than 4Å from the surface vertex were ignored. The default color spectrum used in case of solvent accessibility surface was green, white and blue.

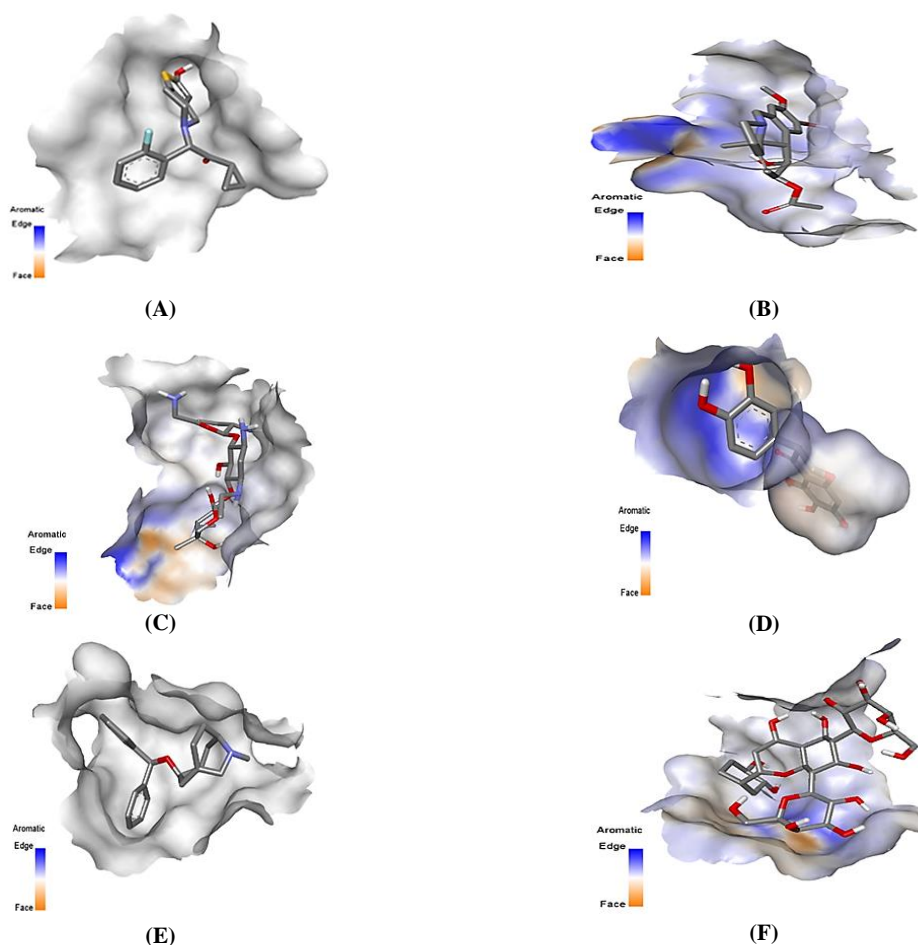


Figure 4. Three dimensional structure analysis of H^+/K^+ -ATPase enzyme and ligand with respect to aromatic edge/face (A) R-95913(B) 2-O-acetylpsuedolycorine (C) netilmicin (D) 5,6,7,3',4',2' pentahydroxyisoflavone (E) benztropine (F) luteolin

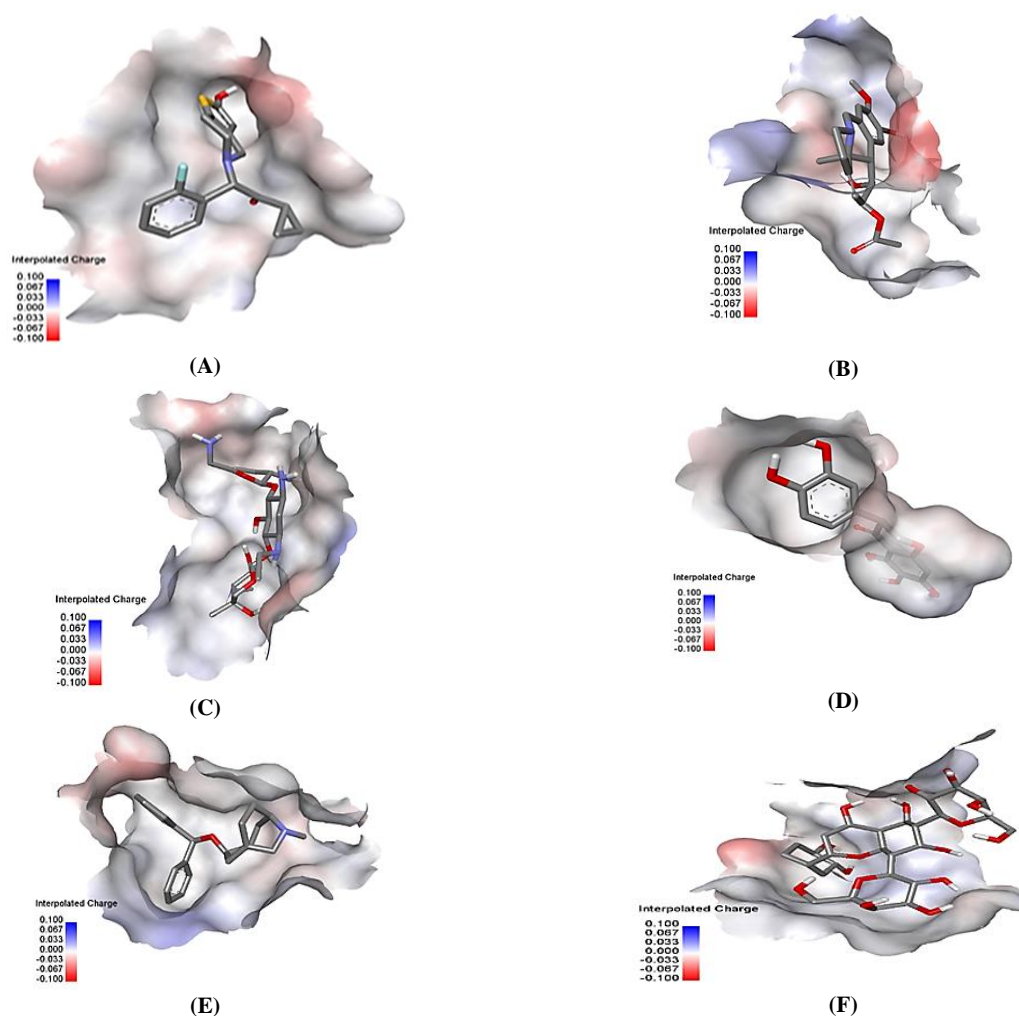


Figure 5. Three dimensional structure analysis of H⁺/K⁺-ATPase enzyme and ligands with respect to interpolated charge(A) R-95913(B) 2-O-acetylpsudolycorine(C) netilmicin (D) 5, 6, 7, 3', 4' pentahydroxyisoflavone (E) benztropin (F) luteolin

The full color map ranged value was 0 to 100. However, it is narrowed to 10.0 to 25.0 by default for improved color contrast. The small value (green) corresponded to buried residue whereas large value (blue) corresponded to exposed residue. Upon folding of a protein, a large fraction of its residue became inaccessible to solvent. Burial of non-polar surface area in the protein interior was an energetically favorable process, and the hydrophobic driving force was one of the most important determinations of protein structure and stability.

Residue burial was conventionally quantitated by a parameter called the solvent accessible surface area [36]. As it is clear in ligand receptor complexes, green areas corresponded to buried residue whereas large blue areas corresponded to exposed residue. The topographical surface area

of ligands R-95913 and 2-O-acetylpsudolycorine was 68.78A² and 182.74A², respectively. The green color in receptor protein complexes indicated a buried region which is present in the upper part of the complex. The topographical polar surface area of the ligand netilmicin, 5, 6, 7, 3', 4' pentahydroxyisoflavone, benzotropine, and luteolin were reported 127.45A², 12.47A², 111.13A², and 107.22A², respectively. The details of topographical polar surface area of ligands are given in supplementary Table 3.

The procedure to arrive at the color of the surface vertices was analogous to the procedure described for the hydrogen bond donor or acceptor. The default color spectrum used was blue, white and brown. The full color map range of value was -4.5 to +4.5. However, it was

narrowed to -3.0 to +3.0 by default for improved color contrast. The hydrophilic residue was represented by a negative value (blue) while the hydrophobic residue was represented by a positive value (brown). The hydrophobic property of H^+/K^+ -ATPase enzyme with six different ligands is depicted in Figure 8. The hydrophobic effect plays a crucial role in driving the thermodynamics of the overall structure of nucleic acids, proteins, and membranes in aqueous environments. This effect is achieved through the burial of hydrophobic groups and the exposure of hydrophilic groups. By minimizing the contact between hydrophobic regions and water molecules, the system achieves a more energetically favorable state, contributing to the stability and organization of these biomolecules in water [37]. As it is clear from the above color spectrum, the blue color indicated hydrophilic residue which was dominant in receptor ligand complexes. Water not only participates as a solvent but as an active matrix since almost all biomolecules are inactive in its absence. Hydration determines their structural stability, dynamics and function in vitro and in vivo [38]. The hydrophilic residue was represented by a

negative value (blue), while the hydrophobic residue was represented by a positive value (brown). In case of ligand R-95913 and receptor protein, the most part was blue which indicated that the major area was hydrophilic in nature.

In the case of the ligand 2-O-acetylpsudolycorine and its receptor protein, the upper part of the receptor protein is indicated as hydrophilic (blue), while the lower part is indicated as hydrophobic. Similarly, in the case of the ligand netilmicin and its receptor protein, the lower area of the receptor protein is also indicated as hydrophobic. This trend of hydrophilic upper parts and hydrophobic lower parts is observed in the ligand 5,6,7,3',4'-pentahydroxyisoflavone-receptor protein complex as well. These observations suggest a consistent pattern in the hydrophilic and hydrophobic characteristics of these ligand-receptor protein complexes, highlighting the importance of such interactions in ligand binding and recognition. In case of ligand benztropine receptor protein, most of the area was brown and white which indicated hydrophobicity which is also given in supplementary Table 3.

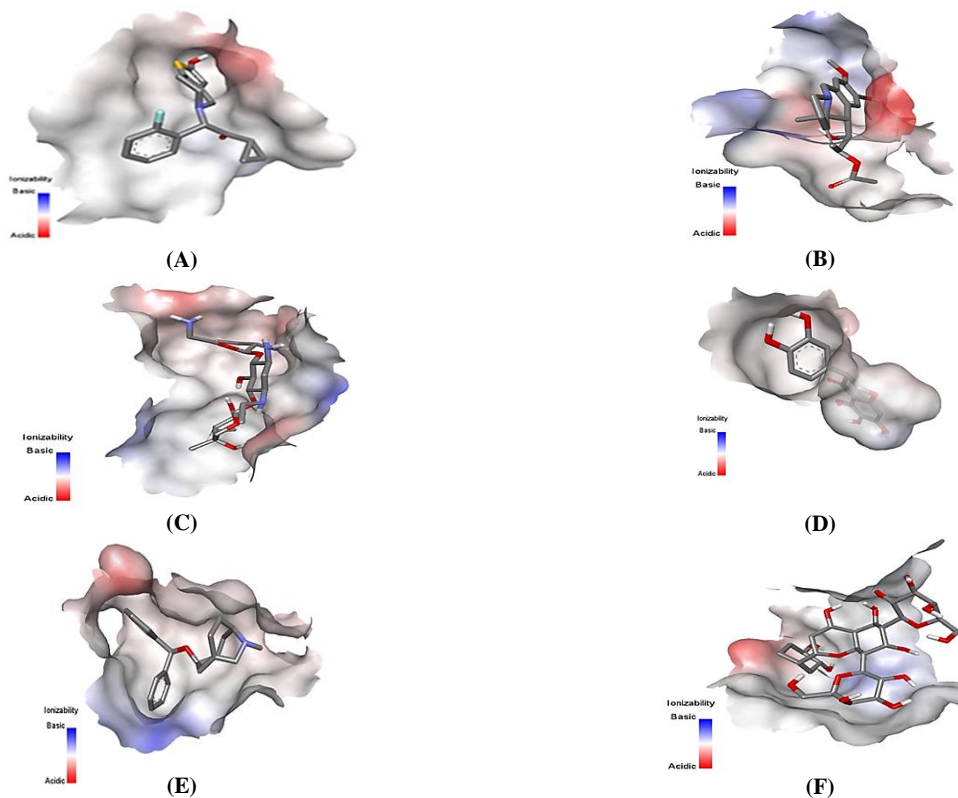


Figure 6. Three dimensional structure analysis of H^+/K^+ -ATPase enzyme and ligand with respect to ionizability (A) R-95913 (B) 2-O-acetylpsudolycorine (C) netilmicin (D) 5, 6, 7, 3', 4' pentahydroxyisoflavone (E) benztropine (F) luteolin

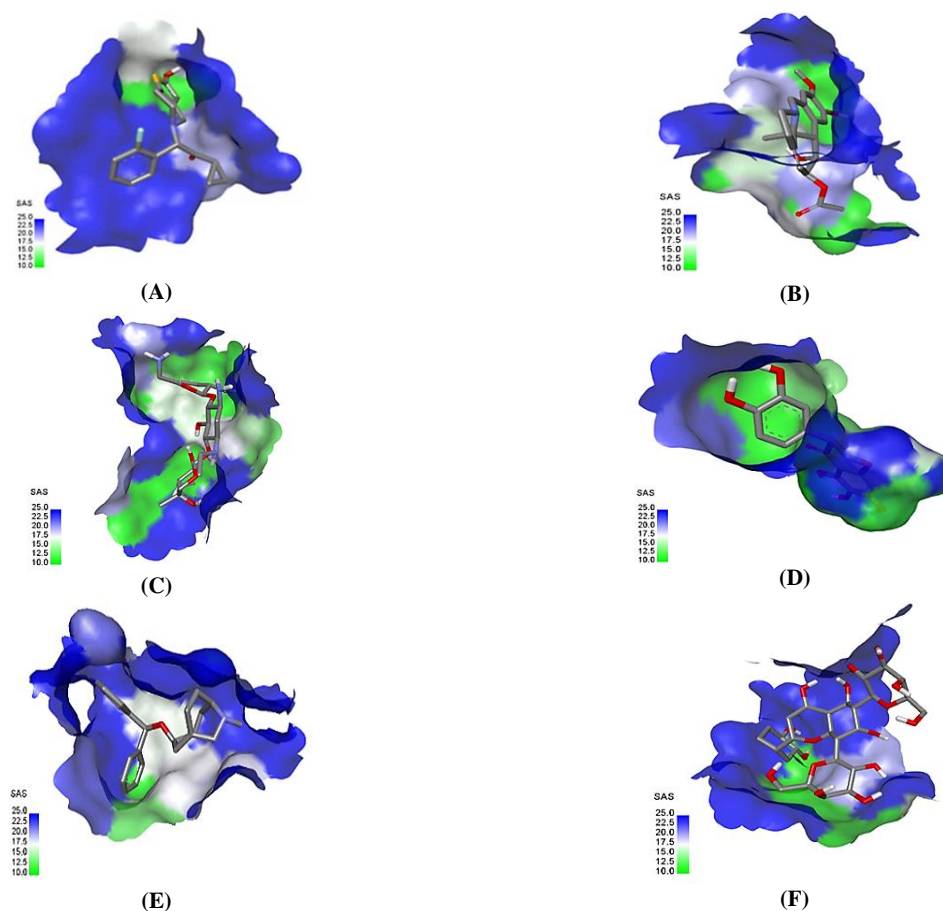


Figure 7. Three dimensional structure analysis of H⁺/K⁺-ATPase enzyme and ligand with respect to solvent accessibility surface (A) R-95913 (B) 2-O-acetylpsuedolycorine (C) netilmicin (D) 5, 6,7, 3,'4,' pentahydroxyisoflavone (E) benzotropine (F) luteolin

The formation of complex with ligand luteolin and receptor protein has predominant blue color that indicates hydrophilic nature. Despite the high binding affinity of the compounds for protein targets, a promising drug candidate should also fulfil the paramount criteria of drug likeness. Drug likeness is only achieved when the molecules and test compounds are under acceptable range. Such features include water solubility, lipophilicity, molecular size, flexibility, polarity and saturation of the compounds. They determine whether a compound will be orally bioavailable or not. Water solubility is associated with lipophilicity and permeability which in turn determine the bioavailability of molecule at the target site [39]. The compounds benzotropine and R-95913 are moderately soluble in water. All six compounds have a good bioavailability score of 0.55. In addition to the drug likeness properties, the pharmacokinetics properties of the compounds were also considered. The results indicated that quercetin might escape the efflux

pump (P-gp) which is a multidrug resistant protein that offers protection to the organ from oxidative damage by xenobiotics. Approximately, 90% of known drugs are substrate of the 5 important isoforms CYP1A2, CYP2C19, CYP2C9, CYP2D6, CYP3A4. Different researchers have previously utilized the ethanol extract of *Piper betle* for the treatment of peptic ulcer. However, in the present study, computational drug design methodologies were employed to identify a phytomolecule that can effectively inhibit the H⁺/K⁺-ATPase enzyme. By utilizing computational approaches, this study aimed to identify a specific phytomolecule that demonstrates promising potential in inhibiting the H⁺/K⁺-ATPase enzyme, which is associated with peptic ulcer pathology. The physicochemical properties like absorption, distribution, metabolism, and excretion of selected phytoconstituents were evaluated by using web tool SwissADME.

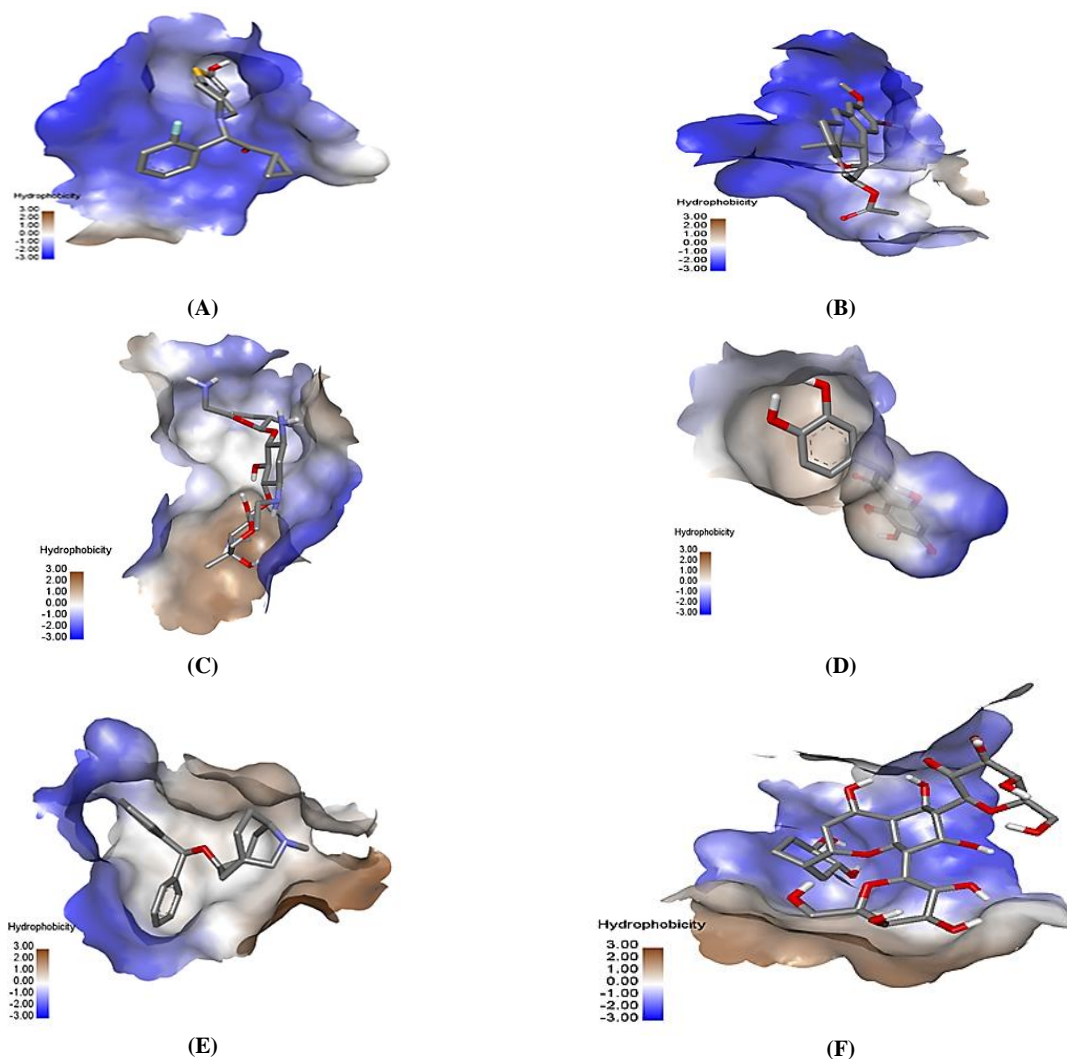


Figure 8. Three dimensional structure analysis of H^+/K^+ -ATPase enzyme and ligand with respect to hydrophobicity (A) R-95913(B) 2-O-acetylpsudolygorine (C) netilmicin (D) 5,6,7,3',4', pentahydroxyisoflavone (E) benzotropine (F) luteolin

Reason behind this evaluation was assessment of competence of dynamic molecules and their strength to reach the target site in bioactive form which involves cellular, animal, and human clinical trials, which are highly priced and encumbered with risk. In the present research, we evaluated the ADME properties of the phytoconstituents of “Magahi pan”, data is given in supplementary Table 3.

The general characteristics of the phytoconstituents of “Magahi pan” revealed that all the six selected phytoconstituents had molecular weight less than 500Da which is the prime property to be called as drug likeness of the small molecules. The lipophilicity characteristics of compounds portray an important role for molecular discovery activities in multifarious domains. The pharmacokinetics

and drug likeness performed using SwissADME showed a high level of GI absorption with R-95913, 2-O-acetylpsudolygorine, benzotropine, 5, 6, 7, 3', 4' pentahydroxyisoflavone, and luteolin. The gastrointestinal absorption of netilmicin was low. The best part of the Swiss ADME model is that it predicts yes or no if compounds under examination have greater probability to be a substrate or non-substrate of P-gp of cytochrome P450 isoenzymes (CYP1A2, CYPC9, CYP2C19, CYP2D6, and CYP3A4). The skin permeability coefficient ($\log K_p$) is determined using a multiple linear regression analysis. It has been observed that the more negative the $\log K_p$ value (with K_p measured in cm^2/sec), the lower the permeability of the molecule through the skin. In other words, molecules with a more negative $\log K_p$ value

exhibit lower permeability and have a reduced ability to penetrate the skin barrier. This relationship between logK_p and skin permeability provides valuable insights into the permeation characteristics of molecules and their potential for transdermal delivery [40].

Among the phytonstituents of “Magahi pan”, R-95913 have (-5.84cm/sec), 2-O-acetylpsuedolycorine have (-8.07cm/sec,) netilmicin have (-11.64cm/sec), 5, 6, 7,3',4' pentahydroxyisoflavone have (-6.84cm/sec), Benzotropine have (-4.82cm/sec) and luteolin have(-6.25cm/sec). It is clear from supplementary Table 3 that netilmicin was the least permeant.

Two molecules, R-95913 and benzotropine, were within yolk regions (high brain penetration regions) and four molecules 2-O-acetylpsuedolycorine, netilmicin, 5,6,7,3',4' pentahydroxyisoflavone and luteolin were in white regions (high passive absorption in GIT regions), respectively. The bioavailability radar enables a first glance at the drug likeness of the molecules. The details of pharmacokinetics property are given in supplementary Table 3.

Conclusion

The study identified specific phytochemicals from *Piper betle* L. var. *magahi* with promising potential as therapeutic agents. The molecules 5,6,7,3',4' pentahydroxyisoflavone and Luteolin showed favorable binding energy and K_i values, indicating their potential efficacy against enzyme H⁺/K⁺-ATPase.

Acknowledgments

The authors are thankful for the facilities provided by the Venture Centre, Pune, India for providing advanced analytical service for LC/MS spectroscopic analysis.

Author contributions

Singh Nadkar Narayan Singh participated in conceptualization, methodology, investigation, writing and editing the original draft; Gurfateh Singh participated in conceptualization and analysis of LC/MS data; Alok Mukherjee and Sailendra Kumar Mahanta participated in molecular docking, data analysis, review and editing the manuscript; Shivnath Das helped in plant authentication and sample preparation for LC/MS.

Declaration of interest

The authors declare that there is no conflict of

interest. The authors alone are responsible for the accuracy and integrity of the paper content.

References

- [1] Sonnenberg A. Epidemiology of *Helicobacter pylori*. *Aliment Pharm Ther.* 2022; 55(S): 1–3.
- [2] Bhatti M, Bhandari DD, Singh J. Review on peptic ulcer and its effective management and treatment with herbals. *Res J Pharm Technol.* 2022; 15(8): 3580–3588.
- [3] Huang D, Lee J, Song N, Cho S, Choe S, Shin A. Gallstones, cholecystectomy and the risk of hepatobiliary and pancreatic cancer: a nationwide population-based cohort study in Korea. *J Cancer Prev.* 2020; 25(3): 164–172.
- [4] Martens E, Demain AL. The antibiotic resistance crisis, with a focus on the United States. *J Antibiot.* 2017; 70(5): 520–526.
- [5] Paranjpe R, Gundala SR, Lakshminarayana N, Sagwal A, Asif G, Pandey A, Aneja R. *Piper betel* leaf extract: anticancer benefits and bio-guided fractionation to identify active principles for prostate cancer management. *Carcinogenesis.* 2013; 34(7): 1558–1566.
- [6] Lubis RR, Wahyuni DD. Antibacterial activity of betle leaf (*Piper betle* L.) extract on inhibiting *Staphylococcus aureus* in conjunctivitis patient. *Am J Clin Exp Immunol.* 2020; 9(1): 1–5.
- [7] Basak S, Guha P. Betel leaf (*Piper betle* L.) essential oil microemulsion: characterization and antifungal activity on growth, and apparent lag time of *Aspergillus flavus* in tomato paste. *LWT.* 2017; 75: 616–623.
- [8] Arawwawala LD, Arambewela LS, Ratnasooriya WD. Gastroprotective effect of *Piper betle* Linn. leaves grown in Sri Lanka. *J Ayurveda Integr Med.* 2014; 5(1): 38–42.
- [9] Perumal PA, Saravanabhavan K. Antidiabetic and antioxidant activities of ethanolic extract of *Piper betle* L. leaves in catfish, *Clarias gariepinus*. *Asian J Pharm Clin Res.* 2018; 11(3): 194–198.
- [10] Ali A, Chong CH, Mah SH, Abdullah LC, Choong TS, Chua BL. Impact of storage conditions on the stability of predominant phenolic constituents and antioxidant activity of dried *Piper betle* extracts. *Molecules.* 2018; 23(2): 484–485.
- [11] Sathi SS, Kiran CN, Santosh F, Fadli A, May F, Ibrahim A, Jiyauddin K. Comparison of wound healing activity of *Piper betle* and

- Ocimum sanctum* in Wistar rats. *Int J Med Toxicol Legal Med.* 2020; 23(1–2): 109–116.
- [12] Biswas P, Anand U, Saha SC, Kant N, Mishra T, Masih H, Bar A, Pandey DK, Jha NK, Majumder M, Das N. Betelvine (*Piper betle* L.): a comprehensive insight into its ethnopharmacology, phytochemistry, and pharmacological, biomedical and therapeutic attributes. *J Cell Mol Med.* 2022; 26(11): 3083–3091.
- [13] Depi S. Review of traditional use, phytochemical and pharmacological activity of *Piper betle* L. *Galore Int J Health Sci Res.* 2020; 5(3): 59–66.
- [14] Nair SS, Kavrekar V. In vitro screening of larvicidal and insecticidal activity of methanolic extracts of *Artocarpus heterophyllus*, *Artocarpus altilis* and *Piper betle*. *Int J Environ Agric Biotechnol.* 2017; Article ID 238672.
- [15] Aara A, Chappidi V, Ramadas MN. Antioxidant activity of eugenol in *Piper betel* leaf extract. *J Family Med Prim Care.* 2020; 9(1): 3–5.
- [16] Pecková R, Doležal K, Sak B, Květoňová D, Kváč M, Nurcahyo W, Foitová I. Effect of *Piper betle* on *Giardia intestinalis* infection in vivo. *Exp Parasitol.* 2018; 184: 39–45.
- [17] Das S, Parida R, Sandeep IS, Nayak S, Mohanty S. Biotechnological intervention in betelvine (*Piper betle* L.): a review on recent advances and future prospects. *Asian Pac J Trop Med.* 2016; 9(10): 938–946.
- [18] Madhumita M, Guha P, Nag A. Bio-actives of betel leaf (*Piper betle* L.): a comprehensive review on extraction, isolation, characterization, and biological activity. *Phytother Res.* 2020; 34(10): 2609–2627.
- [19] Salem MA, Perez de Souza L, Serag A, Fernie AR, Farag MA, Ezzat SM, Alseekh S. Metabolomics in the context of plant natural products research: from sample preparation to metabolite analysis. *Metabolites.* 2020; 10(1): 37–38.
- [20] López-Fernández O, Domínguez R, Pateiro M, Munekata PE, Rocchetti G, Lorenzo JM. Determination of polyphenols using liquid chromatography–tandem mass spectrometry technique (LC–MS/MS): a review. *Antioxidants.* 2020; 9(6): 1–27.
- [21] Gohlke H, Klebe G. Approaches to the description and prediction of the binding affinity of small-molecule ligands to macromolecular receptors. *Angew Chem Int Ed Engl.* 2002; 41(15): 2644–2676.
- [22] Krüger A, Gonçalves Maltarollo V, Wrenger C, Kronenberger T. ADME profiling in drug discovery and a new path paved on silica. [Accessed 2023]. Available from: <https://www.intechopen.com/chapters/66969>.
- [23] Mohapatra RK, El-ajaily MM, Alassbaly FS, Sarangi AK, Das D, Maihub AA, Bengweirif SF, Mahal A, Suleiman M, Perekhoda L, Azam M. DFT, anticancer, antioxidant and molecular docking investigations of some ternary Ni (II) complexes with 2-[(E)-[4-(dimethylamino)phenyl] methyleneamino] phenol. *Chem Papers.* 2021; 75: 1005–1019.
- [24] Okasha RM, Al-Shaikh NE, Aljohani FS, Naqvi A, Ismail EH. Design of novel oligomeric mixed ligand complexes: preparation, biological applications and the first example of their nanosized scale. *Int J Mole Sci.* 2019; 20(3): 1–21.
- [25] Cao X, Tarr MA. Aldehyde and ketone photoproducts from solar-irradiated crude oil–seawater systems determined by electrospray ionization–tandem mass spectrometry. *Environment Sci Technol.* 2017; 51(20): 11858–11866.
- [26] Khanna S, Rao B, Ghosh C, Rizvi Z, Bajaj K, Kulkarni-Almeida A, Sharma R. Discriminating between active and inactive compounds using binding energy calculations, a case study. *Biointerface Res Appl Chem.* 2016; 6: 4–5.
- [27] Li Z, Li X, Huang YY, Wu Y, Liu R, Zhou L, Lin Y, Wu D, Zhang L, Liu H, Xu X. Identify potent SARS-CoV-2 main protease inhibitors via accelerated free energy perturbation-based virtual screening of existing drugs. *Proc Natl Acad Sci USA.* 2020; 117(44): 27381–27387.
- [28] Tan YS, Verma CS. Straightforward incorporation of multiple ligand types into molecular dynamics simulations for efficient binding site detection and characterization. *J Chem Theory Comput.* 2020; 16(10): 6633–6644.
- [29] Hudson KL, Bartlett GJ, Diehl RC, Agirre J, Gallagher T, Kiessling LL, Woolfson DN. Carbohydrate–aromatic interactions in proteins. *J Am Chem Soc.* 2015; 137(48): 15152–15160.

- [30] Rai BK, Bakken GA. Fast and accurate generation of ab initio quality atomic charges using nonparametric statistical regression. *J Comput Chem.* 2013; 34(19): 1661–1671.
- [31] Peluso P, Chankvetadze B. Recognition in the domain of molecular chirality: from noncovalent interactions to separation of enantiomers. *Chem Rev.* 2022; 122(16): 13235–13400.
- [32] Ausaf Ali S, Hassan I, Islam A, Ahmad F. A review of methods available to estimate solvent-accessible surface areas of soluble proteins in the folded and unfolded states. *Curr Pro Pep Sci.* 2014; 15(5): 456–476.
- [33] Zhang J, Chen W, Sun P, Zhao X, Ma Z. Prediction of protein solvent accessibility using PSO-SVR with multiple sequence-derived features and weighted sliding window scheme. *BioData Min.* 2015; 8: 1–15.
- [34] Hong H. Toward understanding driving forces in membrane protein folding. *Arch Biochem Biophys.* 2014; 564: 297–313.
- [35] Bellissent-Funel MC, Hassanali A, Havenith M, Henchman R, Pohl P, Sterpone F, Van Der Spoel D, Xu Y, Garcia AE. Water determines the structure and dynamics of proteins. *Chem Rev.* 2016; 116(13): 7673–7697.
- [36] Wang CK, Craik DJ. Cyclic peptide oral bioavailability: lessons from the past. *Peptide Sci.* 2016; 106(6): 901–909.
- [37] Ranjith D, Ravikumar C. SwissADME predictions of pharmacokinetics and drug-likeness properties of small molecules present in *Ipomoea mauritiana* Jacq. *J Pharmacogn Phytochem.* 2019; 8(5): 2063–2073.
- [38] Kildaci I, Budama-Kilinc Y, Kecel-Gunduz S, Altuntas E. Linseed oil nanoemulsions for treatment of atopic dermatitis disease: formulation, characterization, in vitro and in silico evaluations. *J Drug Delivery Sci Technol.* 2021; Article ID102652.
- [39] Wang CK, Craik DJ. Cyclic peptide oral bioavailability: lessons from the past. *Peptide Sci.* 2016; 106(6): 901–909.
- [40] Zhao H, Liu C, Quan P, Wan X, Shen M, Fang L. Mechanism study on ion-pair complexes controlling skin permeability: effect of ion-pair dissociation in the viable epidermis on transdermal permeation of bisoprolol. *Int J Pharmaceut.* 2017; 532(1): 29–36.

Abbreviations

PUD: peptic ulcer disease; PPIs: proton pump inhibitors; HBPC: hepatic biliary peptic cancers; LC/MS: liquid chromatography mass spectroscopy; ¹H NMR: hydrogen-1 nuclear magnetic resonance; ¹³C NMR: carbon-13 nuclear magnetic resonance; FTIR: Fourier transform infrared spectroscopy; H⁺/K⁺-ATPase enzyme; hydrogen/potassium ATPase enzyme; ESI: electrospray ionization